Christophe GUTFRIND[1,2], Jean-Claude VANNIER[1], Pierre VIDAL[1], Philippe DESSANTE[1]

SUPELEC (1), ELECTRICFIL Automotive (2)

Analytical study of an optimized limited motion actuator used in engine combustive flow regulation

Abstract. *This article aims at an optimal design of a limited motion actuator regulating a flap position in order to control the combustive flow of a diesel engine. The required performances are a reduced size for a 0.4 Nm torque and an angular stroke from 0 to 80°, with operative constraint at 130°C temperature and at 9V voltage. The objective is to minimize the electrical energy consumption of an electromechanical actuator composed by a brushed DC motor and a spur gear set. A finite element model with Flux2D software is used to check the optimized actuator.*

Streszczenie. *Artykuł ma na celu optymalne zaprojektowanie aktuatora z ograniczonym zakresem ruchu, regulującego pozycję wahacza w sterowaniu wydalaniem spalin w silniku diesla. Wymagane działania są zredukowane do momentu 0,4 Nm i kątowego suwu od 0 do 80°, z parametrami działania: temperaturą 130°C i napięciem zasilania 9V. Funkcją celu jest minimalizacja konsumpcji energii elektrycznej w aktuatorze elektromechanicznym złożonym ze szczotkowego silnika prądu stałego i zestawu aktywacji sprzęgła. Zoptymalizowana konstrukcja aktuatora została zweryfikowana modelem numerycznym przy użyciu pakietu FLUX2D. (**Badanie analityczne optymalnego aktuatora z limitowanym ruchem użytego w regulacji wydalania spalin**).*

Keywords: EGR valve, limited stroke, brushed DC motor, spur gear set, optimization.
Słowa kluczowe: zawór EGR, ograniczony suw, szczotkowy silnik prądu stałego, zestaw aktywacji sprzęgłą, optymalizacja.

Introduction

According to the recent European Standard [1] applied to car manufacturers in order to reduce the greenhouse gases and polluting emissions of vehicles, new conceptions of internal combustion engines need a new regulation management of combustive as described in [2].

After a state of the art about several actuators which manage the combustive flow, as shown in [3], two electric topologies to produce rotary movements can mainly be of interest: the first one is an indirect drive composed of a DC motor, as the fig.1, and a two stage reduction gear as the fig.2 ; the second one is a permanent magnet motor direct drive.

Fig.1. Brushed DC motors

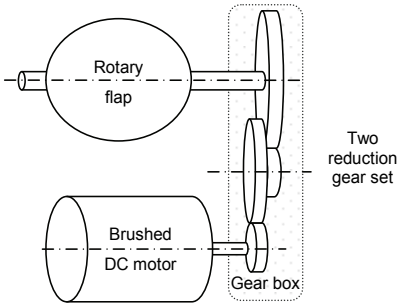

Fig.2. Motor reduction gear unit

The motor reduction gear unit is chosen to be design under constraints. The optimization is realized by genetic algorithm. Magnetostatic and transient studies are carried out with Flux 2D and the gear set freeware with *Filengrene*.

DC motor characterization

The DC motor is structured by one pole pair and two winding paths, according to structures quoted in [4]. Two brushes keep electrical contacts between the stator and the windings paths of rotor. The stator has two permanent magnets and a yoke to drive the magnet and wire created flux.The rotor is composed of *n* turns and steel plates used to drive the flux. Motor model is simplified for analytical modelling and the rotor has ten slots as presented in the following fig.3.

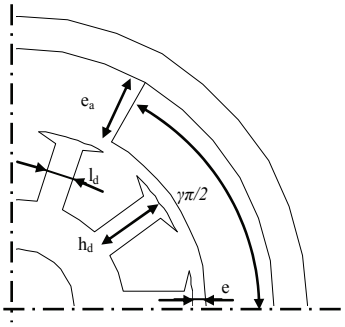

Fig.3. Quarter geometrical brushed DC motor definition

The rotor length is L_r, its radius R_r. The teeth length is h_d, their thickness l_d is defined for a 1.0T flux density. The slot section under pole contains of *n/2* turns in series as :

$$S_{enc} = \frac{N_{enc}}{2} \cdot \left(\frac{\pi \cdot \left(R_r^2 - \left(R_r - h_d \right)^2 \right)}{N_{enc}} - hd \cdot ld \right) \tag{1}$$

Between two brushes, there are two electrical resistances mounted in parallel. Every resistance is composed by *n/2* turns in series. The wire length around one pole is the sum of the length of rotor and the half perimeter concerning the head coil. The electrical resistance is:

$$R = \frac{1}{2} \cdot \rho_{cu} \cdot \left(\frac{n}{2} \cdot \left(L_r + \pi \cdot R_r \right) \cdot \frac{4}{\pi \cdot d_{cu}^2} \right) \tag{2}$$

The rotor is made of steel and copper. The diameter d_{cu} and length wire L_{fil} depends on slot section, electrical resistance and filling factor. The rotor inertia is:

$$J_m = \frac{1}{2} \left(\mu_{fer} \cdot \left(\pi \cdot R_r^2 \cdot L_r - 2 \cdot S_{enc} \right) + \mu_{cu} \cdot \left(\frac{\pi \cdot d_{cu}^2}{4} \cdot L_{fil} \right) \right) \cdot R_r^2 \tag{3}$$

The air gap flux density under a magnetic pole is:

$$B_e = \frac{B_r \cdot e_a}{\mu_a \cdot e + k_{ea} \cdot e_a} \tag{4}$$

With B_r magnet remanent flux density, e_a magnet thickness, μ_a relative permeability, e airgap thickness, and k_{ea} concentration flux density between airgap section and magnet section.

As [4], all wires under a pole induce the back electromotive force. For a pole opening angle $\gamma\pi$ equal to $120/180\pi$, the torque constant is defined by :

(5) $$K_t = 0.5 \cdot \gamma \cdot n \cdot R_r \cdot L_r \cdot B_e$$

In one of the two windings paths, the current value is half of the value that crosses the brush pair. With a current density in slot section J, the nominal torque is defined:

(6) $$C_n = 2 \cdot \frac{J \cdot S_{enc}}{\pi} \cdot B_e \cdot \gamma \cdot \pi \cdot R_r \cdot L_r$$

Then, optimization variables parameters for DC motor are L_r, R_r, h_d, e_a, n, d_{cu}.

Spur gear set definition

The gear set is composed of two stage reduction gears with a 81% efficiency. The gear box reduces speed motor and increases the torque motor with a reduction ratio N between the speed motor ω_m and the flap speed ω_v equal at:

(7) $$\frac{1}{N} = \frac{\omega_v}{\omega_m} = \frac{Z_{1m}}{Z_{2r}} \cdot \frac{Z_{2p}}{Z_{3v}} = \frac{1}{N_{mr}} \cdot \frac{1}{N_{pv}}$$

With Z_p tooth number of motor pinion, Z_r tooth number of intermediate wheel, Z_p tooth number of intermediate pinion, Z_v tooth number of flap wheel.

In order to insure the power transfer between two spur gears as for example pinion motor and intermediate wheel, it is necessary to design the tooth as described in [5,6,7]. The method is based on a study of strength resistance to choose the gear module m_i depending on operating conditions and bending stresses by tangential force F_{ti}. The maximal stress in a tooth must be lower than the elastic stress R_e with a service factor of 25%. Gear material is a Pa 66 with 80MPa elastic strength. The gear thickness is:

(8) $$l_i \geq \frac{54 \cdot F_{ti} \cdot f_s}{R_e \cdot \pi^2 \cdot m_i^2} \cdot m_i$$

Between every stage reduction gear, gear modules must be the same as $m_m = m_r$ and $m_p = m_v$. The tooth thickness is calculated with the maximal transmitting torque. Then the inertia J_{red} of intermediate wheel and pinion can be defined with their thickness and pitch diameters. The total inertia of all moving parts returned on motor shaft J_{tot} can then be calculated:

(9) $$J_{tot} = J_m + \frac{J_{red}}{N_{mr}^2} + \frac{J_{Ch}}{N^2}$$

Consequently, the reduction gear variables parameters are Z_m, Z_r, Z_p, Z_v, m_m, m_p, l_m, l_r, l_p, and l_v.

Dynamics definition

To calculate the flap position versus supply power time, the electrical balance (10) and mechanical (11) equations must be solved. The motor inductance impact is neglected to simplify this calculation as shown in [8].

(10) $$U = R \cdot I + K_e \cdot \omega_m$$

(11) $$J_{tot} \cdot \frac{\omega_m}{dt} = K_t \cdot I - \frac{C_{ch}}{N \cdot r_{red}}$$

According to equations (9) and (10), the load torque on the motor shaft, the motor torque constant and electrical constant, the motor speed are linked by a first order differential equation:

(12) $$\frac{U}{K} - \frac{R \cdot C_{Ch}}{K^2 \cdot N \cdot r_{red}} = \frac{R \cdot J_{tot}}{K^2} \frac{d\omega_m}{dt} + \omega_m$$

To respect constraints, actuator has to drive the flap on 80° angular range, with a 150ms response time including acceleration and deceleration for the forward and backward travel. The optimization method calculate the switching time with respect to the flap position specification on a forward travel of 0° to 80°, and a backward travel of 80° to 0°.
The initial conditions of forward travel being a positive supply voltage U^+ and a null motor speed at 0°, the speed motor during the acceleration time T_a is :

(13) $$\omega_{m-f}^{+}(t) = \left(\frac{U}{K} - \frac{R \cdot C_{ch}}{K^2 \cdot N \cdot r_{red}} \right) \cdot \left(1 - e^{(-t/\Gamma_{em})} \right)$$

With electromechanical constant:

(14) $$\Gamma_{em} = \frac{R \cdot J_{tot}}{K_t^2}$$

In order to obtain a soft landing at 80° flap position, the supply voltage is set at -9V to decelerate the mecanism. The initial condition is the speed given by the preceding speed trajectory and the final condition is a null speed at 80°. The motor speed during the deceleration time is:

(15)
$$\omega_{m-f}^{-}(t) = -\frac{U}{K} - \frac{R \cdot C_{Ch}}{K^2 \cdot N \cdot r_{red}} + \left(\frac{2 \cdot U}{K} - \left(\frac{U}{K} - \frac{R \cdot C_{Ch}}{K^2 \cdot N \cdot r_{red}} \right) \cdot e^{(-T_a/\Gamma_{em})} \right) \cdot e^{(-t/\Gamma_{em})}$$

The backward trip is described by using the same method as for the forward travel. The supply voltage is negative U^- during the acceleration time T_r starting from a null speed motor and at ending maximal speed when the supply voltage is switched to 9V for deceleration time. To obtain the soft landing at 0° flap position, speed motor is:

(16) $$\omega_{m-b}^{-}(t) = -\left(\frac{U}{K} + \frac{R \cdot C_{ch}}{K^2 \cdot N \cdot r_{red}} \right) \cdot \left(1 - e^{(-t/\Gamma_{em})} \right)$$

And the speed motor during deceleration is:

(17)
$$\omega_{m-b}^{+}(t) = \frac{U}{K} - \frac{R \cdot C_{Ch}}{K^2 \cdot N \cdot r_{red}} + \left(-\frac{2 \cdot U}{K} + \left(\frac{U}{K} + \frac{R \cdot C_{Ch}}{K^2 \cdot N \cdot r_{red}} \right) \cdot e^{(-T_r/\Gamma_{em})} \right) \cdot e^{(-t/\Gamma_{em})}$$

For the deceleration time, a simple method calculates the minimal position and the response time must be lower than the 150ms.
Then, the dynamic variables parameters are T_a and T_r.

Electrical energy

Electrical energies are calculated such as for the forward:

(18) $$Ea_f = \int_0^{Ta} U \cdot \frac{U - K_e \cdot \omega_{m-f}^{+}}{R} dt + \int_{Ta}^{T_{stop}} (-U) \cdot \frac{(-U) - K_e \cdot \omega_{m-f}^{-}}{R} dt$$

And the backward:

(19) $$Ea_b = \int_0^{Tr} (-U) \cdot \frac{(-U) - K_e \cdot \omega_{m-b}^{-}}{R} dt + \int_{Tr}^{T_{tp}} U \cdot \frac{U - K_e \cdot \omega_{m-b}^{+}}{R} dt$$

The objective minimizes the mean values of these two trips: $obj = \min\left(mean\left(Ea_f, Ea_b\right)\right)$.

Optimization

Genetic Algorithm (GA) is a sequence of a selection, mutation and crossover of individuals from a population as described in [9] and [10]. An individual is a parameter vector composed by genes. A gene is a variable parameter of actuator such as presented on table 1. Elitism is used to conserve the best individuals of a generation. This strategy copies the best individual from generation $n-1$ into generation n. GA converges to the global best individual who defines the optimized actuator outer constraints and hypothesis.
Contraints and calculation hypothesis are :

- supply voltage 9V
- temperature 130°C

- ferrite magnet with a remanent flux density B_r of 0,4 T and 1,05 relative permeability μ_a
- 0,6 mm for the air gap thickness
- 5 A/mm² current density J in slot section
- rotor radius is 3 times the rotor length
- a filling factor lower than 0,3.

To respect dynamic constraints and to avoid a too restrictive calculation, 5 % tolerance on objective flap position is used during the calculation.

Table 1. Variable parameters of electromechanical actuator

Parameters	Unit	Initial value	Min value	Max value	Optimal value
R_r	mm	12	1	50	10,1
L_r	mm	30	1	50	30,1
e_a	mm	4	1	8	4,7
h_d	mm	4	1	10	4,7
d_{cu}	mm	0,33	0,1	2,5	0,275
n	-	330	1	800	494
T_a	s	0,115	0,01	0,150	0,135
T_r	s	0,07	0,01	0,150	0,065
Z_m	-	11	9	17	11
Z_r	-	55	11	60	55
Z_p	-	11	9	17	11
Z_v	-	57	11	60	53
m_m	mm	1,25	0,5	10	0,8
m_p	mm	2	0,5	10	1,25
l_m	mm	6	2	20	6,63
l_r	mm	7	2	20	8,44
l_p	mm	10	2	20	15,84
l_v	mm	10	2	20	15,74

With initial values, analytical model calculate an actuator consuming a 5,85J mean electrical energy for forward and backward cycle. Optimal values were found by GA at the 2385th generation after 2h computation time. Global optimum is considered reached when the minimal electrical energy no longer varies after 150 generations.

Results

Optimized motor has a torque constant value of 16,8 mN.m/A, a 3.10 ohm electrical resistance value and a $3{,}42.10^{-6}$ kg.m² rotor inertia value. Total inertia value is equal at 4.10^{-6} kg.m².

In the fig.4, for the forward trip, the maximal flap position is 80° at 150 ms and for the backward travel; the minimal flap position is -0,51° at 107 ms.

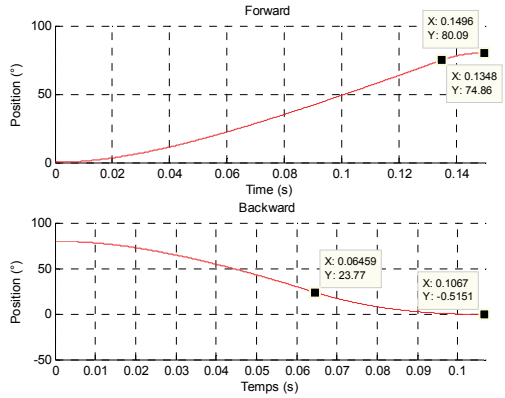

Fig.4 Flap position evolution

DC motor consumes 42W peak electrical power for the forward and 55W for the backward to decelerate the mechanism. The power electronic design could consider these values.

In the fig.5, electrical and mechanical energies are calculated. For the forward trip, the motor consumes 2,47J for the forward travel and 2,12J for the backward trip with a 24,1 gear ratio value. The mean values of electrical energy for forward and backward is 2,3 J.

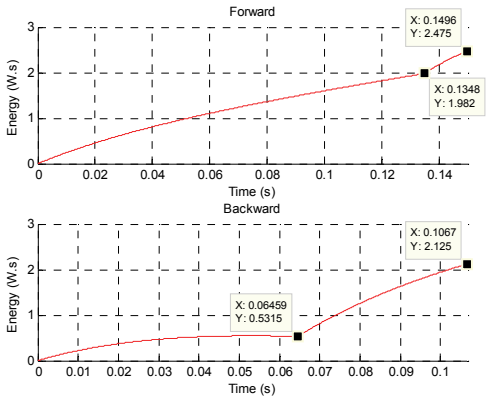

Fig.5 Electrical energy evolution during travels

In the fig.6, to check the electromagnetic behavior of the motor, *Flux-2D* is used with a magnetostatic resolution. The flux density in rotor teeth is equal to 1,0 T.

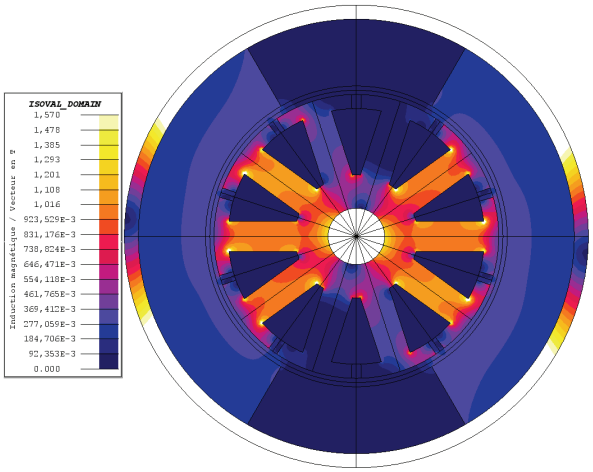

Fig.6 Induction flux density in rotor

In analytical transient behavior, the motor speed maximal value reaches 3033 rpm in forward travel. In fig.7, at 3033 rpm, the motor torque is equal to 19,8 mN.m.

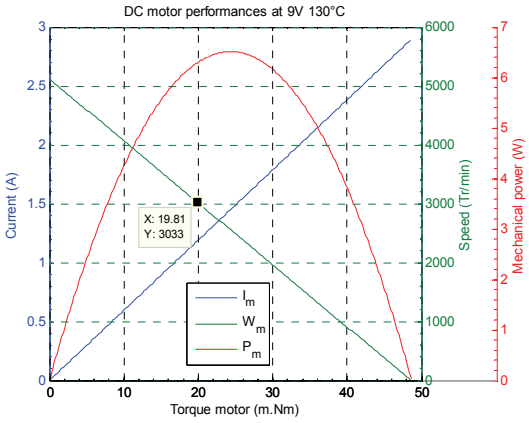

Fig.7 DC motor performances at 9V and 130°C

With the *Flux-2D* transient resolution, in the fig.8, simulation shows a ripple torque while torque values vary between 15 and 20 mN.m.

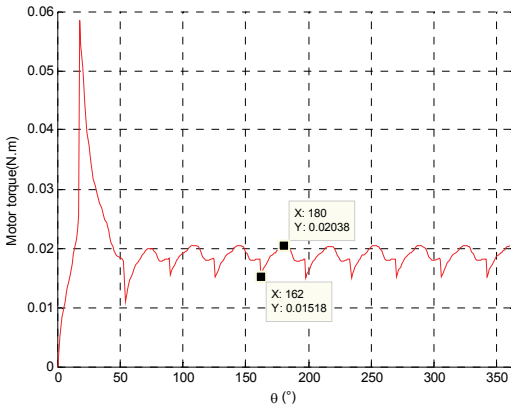

Fig.8 Torque evolution for 3033 rpm speed motor

To verify the optimal DC motor, it is compared with some manufacturer DC motor, as presented in fig.1. Some performances are measured at 25°c and values are shown in the table 2. The optimal motor characteristics are close to the *HC 677* ones.

Table 2. Motor DC performances comparison at 25°c

	Unit	HC 355	SQ2 846	HC 677	HF 383	Optim motor
R	Ω	3,6	3,6	2,3	4,2	2,2
K_t	mN.m/A	17	18	20	19	21,4
J_m	10^{-6} kg.m²	1,39	1,57	3,4	1,45	3,42
Γ_{em}	ms	17	16	21,6	17	18

To respect dynamics, gear teeth are designed with the maximal torque in backward travel. To decelerate the mechanism, motor needs more current for the backward trip because of kinetic energy and the opposite load. As shown in the fig.9, the motor needs 6,07A to develop 0,101N.m.

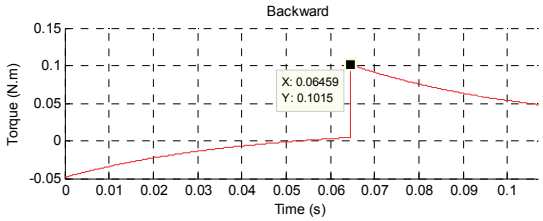

Fig.9 Torque motor evolution during backward trip

As presented in the fig 10, a gear design freeware *Filengrene* [11] can check the geometrical tooth of reduction gear, and operating conditions with calculated parameters.

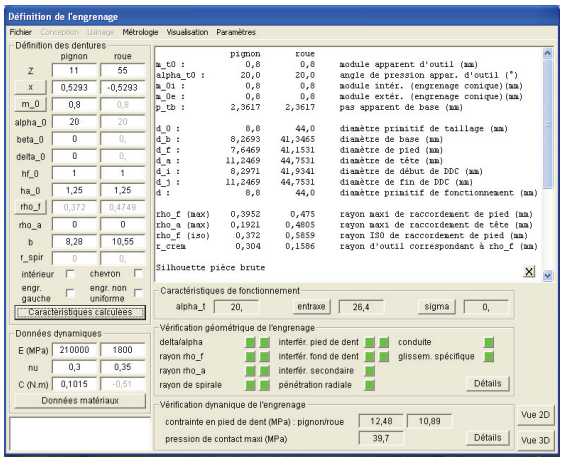

Fig.10 Reduction stage gear checking

From a geometrical point of view, the gear box was well designed as shown for the first reduction stage in fig.11.

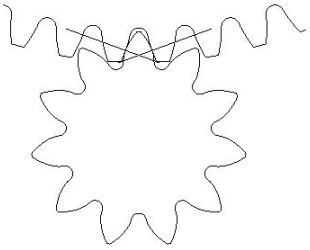

Fig.11 Geometrical gear condition in first reduction stage between motor pinion and intermediate wheel

Conclusion

This article proposes an analytical method to optimize a position actuator including the dynamic response and the spur gear set. After this first electromagnetic and dynamic approach, the machine design can be improved in order to refine the actuator as:

- influence of ripple torque on flap position,
- the self-heating coils on performance actuator.

To continue this optimization, a servo control as [12] is coupled with a position sensor on EGR valve. The next step is to realize a global optimization with power electronic design and feedback position in order to design an electromechanical system.

REFERENCES

[1] European Union Official Journal from European Parliament and Council of 20th June 2007: law (CE) n°715/2007

[2] JUMIN WANG, Air fraction Estimation for multiple combustion mode diesel engines with dual-loop EGR systems, 46th IEEE Conference on decision and control, New Orleans, USA, Dec12-14, 2007, ThPi24.3

[3] D.ILES-KLUMPNER, I.SERBAN, M. RISTICEVIC, "Automotive Electrical Actuation Technologies",IEEE Proceeding. Vehicle Power and Propulsion Conference, (Septembre 2006).

[4] J-C. VANNIER, "Moteurs à courant continu et environnement", Cours Supelec 06825/2001, (2001)

[5] G. HENRIOT, "Engrenages parallèles, Etude géométrique", Techniques de l'ingénieur BM5620 (Juillet 2002)

[6] G. HENRIOT, "Engrenages : détermination des charges sur les dentures et calculs de résistance", Techniques de l'ingénieur BM5623, (Octobre 2002)

[7] G. HENRIOT, "Engrenages parallèles, Dentures corrigées", Techniques de l'ingénieur BM5621, (Juillet 2002)

[8] Wen-Wei CHIANG "Optimal DC motor design for constant voltage seek motion" IEEE transactions on Energy Conversion Vol.5,N°1, March 1990

[9] N. BELLEGARDE, P. DESSANTE, P. VIDAL, J-C. VANNIER, «Optimization of a Drive System and its epicyclic gearset» Intelligent Computer Techniques in Applied Electromagnetics book 07-2008

[10] S.E. SKAAR, R. NILSSEN, «Genetic Optimization of Electric Machines, a state of Art Study»,

[11] André MEYER, Filengrene, http://www.unit.eu/ori-oai-search/notice/view/unit-ori-wf-1-3609

[12] YAODONG PAN, ÜMIT ÖZGÜNER, Variable-structure control of electronic throttle valve, IEEE Transactions on industrial electronics VOL.55 N°11 November 2008

***Authors**: Supélec Ph.D student Christophe Gutfrind for ELECTRICFIL Automotive 77 allée des grandes Combes F-01708 Miribel E-mail: christophe.gutfrind@electricfil.com ; Prof. Dr. Jean-Claude Vannier, E-mail: jean-claude.vannier@supelec.fr ; Prof. Pierre Vidal E-mail: pierre.vidal@supelec.fr ; Prof Dr Philippe dessante E-mail: phillipe.dessante@supelec.fr , Supélec 3 rue Joliot-Curie F-91190 Gif sur Yvette*